

# 1    **The role of stratification on lakes' thermal response: The case of Lake Superior**

2    Sebastiano Piccolroaz<sup>1</sup>, Marco Toffolon<sup>1</sup>, and Bruno Majone<sup>1</sup>

3    <sup>1</sup> Department of Civil, Environmental and Mechanical Engineering, University of Trento, Trento, Italy.

4    Corresponding author: Sebastiano Piccolroaz, Department of Civil, Environmental and

5    Mechanical Engineering, University of Trento, via Mesiano 77, 38123 Trento, Italy.

6    (s.piccolroaz@unitn.it)

## 7    **Abstract**

8    During the last several decades, the Great Lakes region has been experiencing a significant rise in  
9    temperatures, with the extraordinary summer warming that affected Lake Superior in 1998 as an  
10    example of the marked response of the lake to increasingly warmer atmospheric conditions. In this  
11    work we combine the analysis of this exceptional event with some synthetic scenarios, to achieve a  
12    deeper understanding of the main processes driving the thermal dynamics of surface water temperature  
13    in Lake Superior. The analysis is performed by means of the lumped model *air2water*, which simulates  
14    lake surface temperature as a function of air temperature alone. The model provides information about  
15    the seasonal stratification dynamics, suggesting that unusual warming events can result from two  
16    factors: anomalously high summer air temperatures, and increased strength of stratification resulting  
17    from a warm spring. The relative contribution of the two factors is quantified using the model by means  
18    of synthetic scenarios, which provide a simple but effective description of the positive feedback  
19    between the thermal behavior and the stratification dynamics of the lake.

## 1. Introduction

Recent studies have demonstrated that lakes are highly sensitive to changes in environmental conditions, thus representing a valuable proxy to evaluate the effects of a changing climate [Quayle *et al.*, 2002; Adrian *et al.*, 2009; Williamson *et al.*, 2009]. As a consequence, many climate change studies have focused on long-term trends observed in lakes, with particular emphasis on the analysis of water temperature dynamics of large lakes [e.g., Livingstone 2003; Verburg *et al.*, 2003; Vollmer *et al.*, 2005; Coats *et al.*, 2006; Hampton *et al.*, 2008]. Observational evidences revealed that inland water bodies are rapidly warming throughout the world, with Lake Surface water Temperature (LST) increasing at rates up to an order of magnitude higher than those found for the global ocean [Schneider *et al.*, 2009]. Furthermore, it has been shown that lakes warming is in some case larger than that observed for the surrounding air temperature [Austin and Colman 2007; Lenters *et al.*, 2012], especially at mid-latitudes including North America and North Europe [Schneider and Hook, 2010].

Of particular interest is the warming trend that the Laurentian Great Lakes have been experiencing in the last century [e.g., McCormick and Fahnenstiel, 1999]. For example, by using a 100-year long time series of water temperature measured at Lake Superior outlet as a proxy of the offshore LST, Austin and Colman [2008] estimated a mean rate of warming of about  $0.027^{\circ}\text{C yr}^{-1}$  over the last century (i.e., data covering the period 1906-2005), with a dramatic increase up to  $0.11^{\circ}\text{C yr}^{-1}$  taking place starting in the 1980's. This recent trend has been also confirmed by analyzing in situ measurements from offshore buoys [Austin and Colman, 2007]. Notice that these values refer to the three-month summer period July, August and September (JAS), which are the months with the largest LST increases [Lenters 2004; Austin and Colman, 2008]. During the last several decades, similar summer warming trends have been also observed for other lakes in North America, as is the case of Lake Michigan and Lake Huron

42 [Austin and Colman, 2007], and some smaller lakes between California and Nevada [Schneider et al.,  
43 2009]. However, none of these lakes have been showed to warm as rapidly as Lake Superior.

44 In 1998 uncommonly high air temperatures throughout the year determined an exceptional warming of  
45 Lake Superior, with summer LST difference between 1998 and 1997 being higher than the  
46 corresponding air temperature difference. This extraordinary event can be explained as a combined  
47 consequence of a particularly mild, nearly ice-free winter in part due to a significantly strong El Niño  
48 event [Assel et al., 2000; Van Cleave et al., 2014], and an anomalously warm summer season [Austin  
49 and Colman, 2007]. More generally, it can be seen as a remarkable example of the amplified response  
50 of a lake to increasing air temperature, and developing a phenomenological understanding is of  
51 paramount importance for a comprehensive description of lake behavior under evolving climate  
52 conditions. In addition, as water temperature plays a primary role in controlling a wide range of  
53 geochemical and ecological processes, an in-depth analysis of LST dynamics can also provide  
54 significant indirect information concerning possible influences on lake water quality and ecosystem  
55 functioning [e.g., Wetzel, 2001; Winder and Sommer 2012; De Senerpont Domis et al., 2013]. This is  
56 even more relevant considering that an enduring and rapid rising of Lake Superior water temperature  
57 could substantially affect the lake ecosystem [e.g., Magnuson et al., 1997; Cline et al., 2013].

58 Recognizing the main processes affecting the thermal dynamics of LST during an exceptional event  
59 like the 1998 summer warming of Lake Superior can provide a deeper understanding of the thermal  
60 response in more general contexts. A fundamental question, in this perspective, concerns the  
61 contribution to LST variation which is attributable to the increased heat flux in the summer period as  
62 opposed to the influence of previous conditions of the lake. To address such an issue, we exploited  
63 *air2water*, a simple model [Piccolroaz et al., 2013; Toffolon et al., 2014] that simulates LST relying  
64 solely on air temperature, to isolate the relative contributions of two factors: external forcing and

65 thermal structure of the lake. After introducing the model in the next section, we show that these  
66 factors are sufficient to suitably reproduce the LST dynamics, and then we analyze some synthetic  
67 scenarios to isolate their relative importance. Wider implications of the results and conclusions are  
68 finally presented in the last two sections.

## 69 **2. Material and methods**

### 70 *2.1 Study site and available data*

71 Lake Superior (Figure 1) is the largest of the five Great Lakes of North America, and the largest  
72 freshwater basin on Earth by surface area (surface area 82 103 km<sup>2</sup>; volume: 12 000 km<sup>3</sup>; maximum  
73 depth: 406 m). Long-term data of air and surface water temperature are available and are freely  
74 distributed by the National Oceanic and Atmospheric Administration (NOAA).

75 Two different sources of data have been used in this work: daily in situ measurements of air  
76 temperature provided by the National Oceanic and Atmospheric Administration's (NOAA) National  
77 Data Buoy Center (NDBC, webpage: <http://www.ndbc.noaa.gov/>), and daily LST retrieved  
78 from satellite imagery provided by NOAA Great Lakes Environmental Research Laboratory (GLERL,  
79 webpage: <http://www.glerl.noaa.gov/>). Air temperature data adopted in this study are measured at the  
80 STDM4 – Stannard Rock station, which belongs to the NOAA NDBC Coastal Marine Automated  
81 Network (C-MAN) and is installed at about 35 m above the lake level on a lighthouse located in the  
82 South-Eastern part of the lake (see Figure 1). The values of LST freely downloadable by the GLERL  
83 website refer to satellite-derived LST averaged over the whole lake, do not present significant gaps,  
84 and provide information during the entire year. Local LST values of the GLERL dataset are in overall  
85 good agreement with LST measured by offshore buoys (NDBC network) [Schwab *et al.*, 1999], making  
86 the first dataset preferable compared to in situ NDBC measurements, which are characterized by  
87 systematic gaps from October to April when devices are removed to prevent damage from ice. We

88 remark that LST data during winter time are of pivotal importance in order to investigate the role of ice  
 89 in controlling the timing and intensity of LST warming in summer. Both air temperature and LST data  
 90 have been downloaded for the period between 1994 and 2011.

## 91 *2.2 air2water: a simple model to predict LST*

92 The analysis presented in this work has been performed by means of *air2water* [Piccolroaz *et al.*,  
 93 2013], a simple lumped model that allows for estimating LST using air temperature as the only  
 94 meteorological forcing. *air2water* is derived from the volume-integrated heat equation applied to the  
 95 upper layer of the lake

$$96 \quad \rho c_p V_s \frac{dT_w}{dt} = A \Phi_{net}, \quad (1)$$

97 where  $\rho$  is water density,  $c_p$  is the specific heat capacity,  $V_s$  is the surface volume of water that is  
 98 involved in the heat exchange with the atmosphere,  $T_w$  is LST,  $t$  is time,  $A$  is the surface area of the  
 99 lake and  $\Phi_{net}$  is the net heat flux into the upper water volume (accounting for the main fluxes entering  
 100 and exiting  $V_s$ : short and long wave radiation, sensible and latent heat fluxes). After introducing  
 101 appropriate simplifications, which are summarized in Appendix A (for a thorough discussion we refer  
 102 to Piccolroaz *et al.*, [2013] and Toffolon *et al.*, [2014]), the equations of the model in its full (8-  
 103 parameters, from  $a_1$  to  $a_8$ ) version reads as follows:

$$104 \quad \frac{dT_w}{dt} = \frac{1}{\delta} \left\{ a_1 + a_2 T_a - a_3 T_w + a_5 \cos \left[ 2\pi \left( \frac{t}{t_y} - a_6 \right) \right] \right\}, \quad (2)$$

$$105 \quad \begin{cases} \delta = \exp \left( -\frac{T_w - T_h}{a_4} \right) & \text{for } T_w \geq T_h \\ \delta = \exp \left( -\frac{T_h - T_w}{a_7} \right) + \exp \left( -\frac{T_w}{a_8} \right) & \text{for } T_w < T_h \end{cases} \quad (3)$$

106 where  $T_a$  is air temperature,  $\delta$  is a dimensionless number given by the ratio between the volume  $V_s$  of  
 107 the surface layer introduced in equation (1) and a reference volume  $V_r$ , and  $T_h$  is a reference value of

108 the deep water temperature, which is approximately  $4^{\circ}\text{C}$  for deep dimictic lakes. We note that  $V_s$   
109 (hereafter referred to as the reactive volume) varies in time due to thermal stratification, while  $V_r$  is the  
110 maximum volume affected by the surface heat flux when the lake experiences the weakest stratification  
111 conditions. In our formulation these two volumes and the surface heat flux are not estimated separately,  
112 and the parameter  $\delta$  is used to implicitly account for temporary reduction or enhanced efficiency of the  
113 heat exchange with the atmosphere (for instance in the case of ice cover), as will be discussed later on.

114 The model parameters  $a_1$  to  $a_8$  account for a series of different processes and are defined within a  
115 physically reasonable range of variation, and are obtained through calibration against LST  
116 measurements. The ordinary differential equation (2) is solved numerically using the Runge-Kutta  
117 fourth order scheme, with a daily time step. In spite of the simple formulation and the limited number  
118 of parameters, *air2water* is able to satisfactorily capture seasonal variations and inter-annual dynamics  
119 in LST (see *Toffolon et al.*, [2014] for an application of the model to 14 temperate lakes with different  
120 morphological characteristics), thus representing an appealing tool for both conceptual studies and real  
121 case analyses. The fact that the model is data-driven, while being physically based, allows for the direct  
122 acquisition of information about the studied system during the calibration phase, which is performed  
123 via an automatic optimization procedure. Besides predicting LST, the model also estimates the seasonal  
124 evolution of the upper volume of water affected by the surface heat budget, through the evaluation of  
125 the volume ratio  $\delta$  (well-mixed  $\delta \rightarrow 1$ , stratified  $\delta \rightarrow 0$ , ice covered  $\delta > 1$  [*Piccolroaz et al.*, 2013]). The  
126 model has been successfully applied using different sources of data (i.e., LST measured at buoys or  
127 retrieved from satellite) and considering different case studies [*Piccolroaz et al.*, 2013; *Toffolon et al.*,  
128 2014].

### 129 3. Results

### 3.1 Model performances

Model parameters have been calibrated considering the historical series of air temperature and LST available for the period 1994-2011. A general good agreement between measured and simulated series has been obtained, with a Kling Gupta Efficiency (KGE) index [Gupta *et al.*, 2009] of 0.98 and a root mean square error of about 1.1°C. We recall that KGE ranges from  $-\infty$  to 1: the closer to 1, the better the model performances. The mean deviation between simulated and observed LST is equal to -0.0004°C, suggesting the absence of a significant bias. We notice that the performance achieved by *air2water* is fully comparable to that obtained with more complex process-based models [e.g., Thiery *et al.*, 2014], which however require a significantly larger amount of input data.

Figure 2a shows air temperature and LST records for the summer season (averages over JAS). Detecting long-term trends by means of linear regressions is difficult and may lead to results that are not statistically significant. Anyway, it is interesting to note that a significant warming of about 0.098°C yr<sup>-1</sup> ( $R^2 = 0.17$ ,  $p$ -value = 0.09) and 0.107°C yr<sup>-1</sup> ( $R^2 = 0.08$ ,  $p$ -value = 0.27) can be observed for measured air temperature and LST, respectively. This result differs from previous analyses [Austin and Colman, 2007; Schneider and Hook, 2010], which found that LST increased faster than air temperature based on meteorological stations located within a 500 km radius from the lake. Notice that in the present work we refer to air temperature data retrieved at about 35 m above the lake surface from a single station at an offshore location (i.e., STD4 C-MAN station), which is more representative of the real lake conditions, while being fully representative of the typical seasonal thermal pattern of the atmosphere. In fact, the marked time lag between the temporal variations of air and water temperatures is clearly demonstrated in Figure 2b for the two years 1997 and 1998. Figure 2 also shows the performance of the model, which behaves properly both in detecting the long-term LST trend (0.100°C yr<sup>-1</sup>,  $R^2 = 0.13$ ,  $p$ -value = 0.14) and the associated intra- and inter-annual variations. In particular, the two years have been characterized by substantial differences (Figure 2b): 1997 being particularly cold,

154 especially in summer, and 1998 showing unusually warm temperatures during the whole year (as  
155 already discussed above). These marked differences are also evident in Figure 2a, where both JAS air  
156 temperature and JAS LST are positioned below and above the corresponding trend lines, respectively  
157 for 1997 and 1998. In this perspective, this two-year period constitutes an interesting example of inter-  
158 annual climate variability, which is worth being examined to characterize the general thermal dynamics  
159 of the lake.

160 In Figure 3 we show the capability of *air2water* to reliably reproduce the temporal evolution of the  
161 reactive surface volume. This is done by comparing the simulated dimensionless volume ratio ( $\delta_{sim}$ )  
162 (see Section 2.2) with an independent estimate of the same variable ( $\delta_{est}$ ) obtained from the analysis of  
163 water temperature profiles measured at a mooring station deployed in the central part of the lake [Titze  
164 and Austin, 2014]. Water temperature data cover the period 2008-2011 with hourly resolution, and are  
165 available at different depths, from surface down to 250 m depth. Following the same procedure adopted  
166 in Toffolon *et al.*, [2014] for the case of Lake Constance, we used the measured vertical profiles of  
167 temperature to estimate the volume of the surface well-mixed layer, assuming that this is a reasonable  
168 approximation of the reactive volume  $V_s$ . We first identified the thickness of the surface well-mixed  
169 layer as the smallest depth where water temperature difference with respect to surface is lower than a  
170 threshold of 1°C. Then we converted this depth into the corresponding volume of water on the basis of  
171 the hypsometric curve of the lake. Finally, we calculated  $\delta_{est}$  by normalization to a reference volume,  
172  $V_r$ , here assumed to be the entire volume of the lake. Despite the temperature threshold and the  
173 reference volume are arbitrary and may influence the evaluation of  $\delta_{est}$ , the overall comparison  
174 between simulated and estimated  $\delta$  (Figure 3) clearly shows that the simple parameterization (2b) is  
175 able to correctly reproduce seasonal and inter-annual (see e.g., the anticipated stratification in summer  
176 2010) patterns of stratification, thus indicating its suitability to be used for the purposes of this work. In  
177 order to make the comparison between  $\delta_{sim}$  and  $\delta_{est}$  fair, we have calibrated the model locally using



178 LST retrieved from the closest NDBC buoy (i.e., station 45001, located at 2 km from the mooring  
179 station, and for which a 27-year long dataset is available during the period 1985-2011) instead of the  
180 lake-averaged, satellite-retrieved LST. We note that this longer LST series was required to achieve a  
181 more robust calibration of the model than the one that could be obtained relying only on the 4-year data  
182 measured at the thermistor chain. Model calibration over the 27-year period yielded  $KGE = 0.98$ , a  
183 root mean square error of  $1.6^{\circ}\text{C}$ , and mean deviation of  $-0.0086^{\circ}\text{C}$ . In addition,  $\delta_{sim}$  in Figure 3 has  
184 been calculated through equation (3) with the same surface  $T_w$  used to evaluate  $\delta_{est}$ , and the values of  
185 the parameters  $a_4$ ,  $a_7$  and  $a_8$  derived from point calibration of the model.

186 Although  $\delta_{sim}$  is defined as the dimensionless reactive volume, it implicitly accounts for possible  
187 increase or decrease of heat fluxes due complex processes that are not explicitly included in the simple  
188 formulation of the model. For instance, this is the case of the insulating effect of ice cover that results  
189 in a fictitious larger reactive volume (i.e.,  $\delta > 1$  as discussed in *Piccolroaz et al.*, [2013]), or the  
190 increased effective heat fluxes due to unstable atmospheric boundary layer in late summer [*Blanken et*  
191 *al.*, 2011; *Lofgren and Zhu*, 1999] that can be partially explained with the lower values of  $\delta_{sim}$   
192 compared to  $\delta_{est}$  in Figure 3. These results indicate that *air2water* is able to accurately simulate  
193 thermal and stratification dynamics of the lake, without the need to introduce a complex description of  
194 the air-water interface processes based on the quantification of the single heat flux components. This  
195 should be seen as a major advantage of the proposed formulation rather than a limitation, as it is  
196 generally difficult to find complete datasets of all meteorological variables (e.g., solar radiation,  
197 cloudiness, humidity, etc.) covering long-term periods, compared to the relatively larger availability of  
198 air and water temperature measurements.

### 3.2 Assessing the roles of air temperature and stratification

The analysis of the heat balance equation is a good starting point for understanding the influence of stratification, in general, and for pointing out the significant differences between LST in 1997 and 1998 (Figure 2), as a particular case. Looking at equation (1), it is evident that the warming rate of the lake is directly proportional to  $\Phi_{net}$  and inversely proportional to  $V_s$ . The lake warms faster if the heat flux is high and the volume that directly participates in the heat exchange with the atmosphere is small (i.e., the lake is stratified). This is a central feature of the thermal dynamics of lakes.

In order to understand the role of the main factors controlling LST, in Figure 4 we compare the model results obtained for 1997, 1998 and for the mean year (corresponding to the overall period 1994-2011). The analysis of temperature as a function of the day of the year starting from 1 January (Figure 4a) shows again that 1997 and 1998 were respectively colder and warmer than the mean year both concerning air (thin lines) and water (thick lines) temperatures. Figure 4b shows the variation of the volume ratio  $\delta$  calculated for the same three annual cycles. The nearly ice-free winter that occurred in 1998 is reproduced by the model with values of  $\delta$  always  $\sim 1$  (we recall that  $\delta > 1$  accounts for the insulating effect due to the presence of ice). This is confirmed in Figure 4a, where simulated LST is shown to be consistently greater than  $0^\circ\text{C}$  in winter 1998 and did not drop beneath  $\sim 2^\circ\text{C}$  from the end of January to the end of April (contrary to the mean year). Thus, direct thermal stratification in 1998 started about 30 days earlier (start of May) than in 1997 (start of June), and about 20 days earlier compared to the mean year (end of May). Moreover, a significantly faster increase of LST characterized the lake in summer 1998: starting from June (in 1997 during the same period the lake was still inversely stratified, i.e.,  $\text{LST} < 4^\circ\text{C}$ ) the lake reached a sufficiently strong thermal stratification that caused the surface mixed layer to get significantly shallower at mid-July (i.e.,  $\delta \ll 1$ ). Strong stratification conditions, much stronger than those usually characterizing the lake (i.e.,  $\delta_{1998} < \delta_{my}$ , where the subscript ‘my’ stands for mean year), lasted for about 2.5 months, until the start of October.

223 Later on, stratification progressively weakened, but remaining always slightly stronger than in 1997  
224 and in the mean year. As a consequence of the smaller surface volume in September 1998, the decrease  
225 of LST was faster in 1998 than in 1997.

226 As a whole, the combination of an exceptionally high air temperature and a significantly longer period  
227 of thermal stratification in summer 1998 resulted in a higher heat input to the lake acting on a smaller  
228 water volume, and eventually in the significant warming of LST. The onset of stratified conditions was  
229 anticipated, consistently with the observed tendency towards a longer ice-free season in North  
230 American lakes (earlier occurrence of ice-departure dates, see e.g., *Anderson et al.*, [1996]; *Schindler et*  
231 *al.*, [1996]; *McCormick and Fahnenstiel* [1999]). This fact established a positive feedback to LST  
232 warming through an earlier reduction of the surface volume (lower values of  $\delta$ ) and hence a faster  
233 increase of LST, which in turn contributed to further decrease  $\delta$  during summer months.

234 Aimed at understanding the feedback between net heat flux and thermal stratification and evaluating  
235 their distinct contributions to LST dynamics, we applied *air2water* under six different synthetic  
236 conditions, which are summarized in Table 1. In all cases, we considered the same model parameter  
237 set, as identified by calibration over the period 1994-2011. The six cases are described in the following  
238 paragraphs. In the analysis of the results we always refer to JAS as summer period to be consistent with  
239 previous analyses [*Austin and Colman*, 2008; *Van Cleave et al.*, 2014], although we will discuss the  
240 distinct role of the different months, and especially of July, on the average value.

241 Test 1 is obtained by combining air temperature series measured in 1998 and  $\delta$  as simulated for 1997  
242 (i.e.,  $\delta$  is not calculated by the model but externally imposed). The resulting annual cycle of LST is  
243 shown in Figure 4a. Although the external forcing (i.e., air temperature) is the same as in 1998, LST  
244 exhibits a significantly different behavior compared to that simulated for 1998, solely as a consequence  
245 of the different stratification conditions that have been imposed. The timing is similar to that simulated

246 for 1997 (e.g., summer peak around the 20<sup>th</sup> of August) because it is controlled by the value of  $\delta$ ;  
247 moreover, until the end of August LST is generally much lower than in 1998. The mean LST during  
248 JAS is about 1.7°C colder than in 1998, with most of the difference occurring in July (almost 5°C, see  
249 Table 2). In winter, LST for Test 1 is similar to 1998, and the two series start to diverge only when the  
250 stratification begins to play a role. In fact, the lower temperatures in summer for Test 1 can be fully  
251 attributed to the slower warming caused by the larger volume of water involved in the heat exchanges,  
252 and hence to a weaker and postponed thermal stratification of the lake (i.e., larger values of  $\delta$ )  
253 compared to 1998. Finally, Test 1 shows a slower cooling of LST in autumn with respect to 1998. This  
254 indicates a higher thermal inertia of the lake, coherently with the occurrence of larger values of  $\delta$ , thus  
255 larger volumes of water participating to the heat exchanges with the atmosphere.

256 Test 2 is the reciprocal of Test 1 (see Table 1), being obtained by combining air temperature series  
257 measured in 1997 with  $\delta$  simulated for 1998. The analysis of results, which are shown in Figure 4a and  
258 summarized in Table 2, leads to similar, and in some cases complementary, considerations as those  
259 made for Test 1: i) the timing of LST is driven by  $\delta$ , thus is consistent with that simulated for 1998; ii)  
260 the mean LST during the JAS period is about 1.7°C warmer than in 1997, but it is colder than in 1998  
261 and Test 1; iii) July is the month characterized by the largest difference with respect to thermal  
262 conditions in 1997; iv) from June to September the mean monthly LST is always colder than in Test 1  
263 with the exception of July, when the presence of a strong stratification (i.e., small values of  $\delta$ )  
264 determines a faster warming of the lake; and v) in autumn LST decreases faster than in 1997 due to the  
265 reduced thermal inertia of the system (lower values of  $\delta$ ).

266 The combined analysis of Test 1 and Test 2 provides interesting elements for an approximate  
267 quantification of the specific role that net heat flux and stratification play in controlling LST dynamics.  
268 Results in Table 2 suggest that the difference between mean summer (JAS) LST in 1998 and 1997 (i.e.,

about 4.2°C) is attributable to a warmer  $T_a$  for about 60% (the difference between mean summer LST in Test 1 and 1997 is about 2.5°C), and to a stronger stratification for the remaining 40% (the difference between mean summer LST in Test 2 and 1997 is about 1.6°C). We notice that this proportion is valid only for the comparison between 1997 and 1998, and may change in other cases due to the inherent inter-dependence of the two effects and the high non-linearity of the processes involved. However, the results of this simple analysis provide a clear indication that air temperature and thermal stratification play a nearly balanced role in regulating LST behavior.

### 3.3 Assessing the role of the history of the system

Two additional synthetic tests have been built as combinations of  $T_a$  observed in 1997 and in 1998 (see Table 1), aimed at understanding the relative contribution of winter/spring and summer seasons to the 1998 summer warming. In particular, Test 3 has been defined assuming  $T_a$  from 1997 for the period January-June and October-December, and  $T_a$  from 1998 for the remaining period (i.e., JAS). Thus, this synthetic year is characterized by a warm summer and cold conditions during the rest of the year, with steeper rising and falling limbs during June and October, respectively (see Figure 5a). The second synthetic year (Test 4) has been constructed as the opposite to Test 3, thus is characterized by a cold summer ( $T_a$  from 1997) and warm conditions during the rest of the year ( $T_a$  from 1998), with a flatter transition during later spring and early autumn (see Figure 5a). Unlike the previous tests,  $\delta$  is calculated by the model rather than being externally imposed.

Results for Test 3 (Figure 5) show that water temperature remains low from January to June (when the forcing coincides with that observed in 1997), but the lake starts warming as soon as air temperature rises in summer, and eventually in August and September it reaches temperatures that coincide with those obtained in 1998 (see Table 2). This is a consequence of the fact that the late summer/early autumn period is characterized by a strong thermal stratification, thus very small values of  $\delta$ , which

determines a fast adaptation of LST to air temperature [Toffolon *et al.*, 2014], fully overcoming the low temperatures resulting from the colder winter months. On the contrary, the results of the second synthetic year (Test 4, Figure 5) shows that, although LST coincides with that obtained in 1998 from January to June because the external forcing is the same, it starts deviating from the trend observed in 1998 as soon as the colder summer begins. The abrupt warming of the lake is absent, as is suggested by the fact that water temperature does not reach the same maximum of 1998, not even that of the mean year. Nevertheless, LST in summer is always higher than that obtained in 1997 (with the exception of September, when LST coincides in the two cases, see Table 2), coherently with the occurrence of lower (or at least equal) values of  $\delta$  throughout the whole year.

The comparison between the mean summer values of LST reported in Table 2 shows that the lake in Test 3 is about 2.6°C warmer than in 1997, which allows one to conclude that the exceptionally high air temperatures registered during the JAS period in 1998 alone contributed to about 60% of the whole LST difference between 1998 and 1997 (i.e., nearly 4.2°C). Analogously, from Test 4 we can infer that the occurrence of a warm winter/spring period in 1998 alone explained about 40% (i.e., about 1.7°C) of the total mean summer LST difference between the two years. It is necessary to notice that although the two contributions sum to almost 100%, this is purely due to how scenarios have been constructed, and should not be taken as general rule.

The thermal response of lakes is strictly dependent on the sequence of meteorological and climatic conditions, thus making difficult to analyze the independent contributions of single periods of the year. This is especially true for deep lakes during non-stratified or weakly stratified conditions, when, thanks to a high thermal inertia (large volume of the surface layer, i.e. large  $\delta$  in our model), the system is able to retain a historical memory of the past conditions, with a significant influence on the ensuing thermal dynamics. Conversely, during the stratification period, the response time of LST to changes in air

315 temperature is shortened considerably due to the low thermal inertia [Toffolon *et al.*, 2014]. Hence, the  
316 adaptation of LST to air temperature is more rapid and its variation more intense, with the inertial  
317 effect being significantly reduced during strong stratification conditions.

318 The behavior discussed above is quantitatively analyzed in the last two synthetic tests (Figure 6), which  
319 rely on an ensemble of 365 air temperature cycles dynamically reconstructed on the basis of two  
320 reference years: a warm year and a cold year. The air temperature in the colder year has been fixed as  
321 in the mean year 1994-2011 ( $T_{my}$ ), while the warmer year has been defined as  $T_{my} + \Delta T_a$ , where the  
322 increment  $\Delta T_a$  has been assumed equal to the average difference between 1998 and the mean year,  
323 which is approximately 2°C.

324 The 365 annual cycles of air temperature used in Test 5 have been obtained by combining the first part  
325 of the warm year with the remaining part of the cold year, progressively delaying by one day the  
326 transition between the warm and cold conditions, from January 1 to December 31 (see Figure 6a for a  
327 schematic illustration). Test 5 is thus aimed at quantifying the effect that a lasting warm winter may  
328 produce on the annual evolution of LST. Test 6 is the opposite case of Test 5 (see Figure 6b) and is  
329 aimed at evaluating the possible effect of an anticipated warm summer. Therefore, Tests 5 and 6, in  
330 addition to Tests 3 and 4, contributes to a comprehensive overview of the possible effects that different  
331 air temperature conditions, occurring at different times of the year, may have on LST dynamics.

332 We focused on the analysis of LST changes during five different periods of the year: June, July,  
333 August, September, and the entire summer period JAS. For each of these periods, we evaluated the  
334 difference  $\Delta T_w$  between the period-averaged LST of the test and of the mean year, and we plotted it as  
335 a function of the  $i$ -th day of the year when the transition between the two reference years takes place  
336 (Figure 6c-g):

$$\Delta T_w|_{t_1}^{t_2}(i) = \frac{1}{(t_2 - t_1)} \left[ \int_{t_1}^{t_2} T_w^{test(i)} dt - \int_{t_1}^{t_2} T_w^{my} dt \right], \quad (4)$$

where  $t_1$  and  $t_2$  are the limits of the averaging period (delimited by vertical lines in Figure 6c-g),  $T_w^{my}$  is the LST calculated for the mean year, and  $T_w^{test(i)}$  is the LST calculated for each case  $i$  of the set of 365 annual cycles of air temperature constituting the two tests (Figure 6a-b). Continuous ascending and descending curves in Figure 6 refer to Test 5 and Test 6, respectively.

These plots provide an immediate picture and a quantitative evaluation of the effects that a progressive shift of the transition between the two reference years may have on the mean LST. In particular, we analyzed five target periods of the year previously identified (i.e., the single months June, July, August, September, and the summer period JAS, see Figure 5 from subplot c to subplot g). In order to correctly interpret the figure, we suggest to read the ascending curve from left to right (i.e., LST increases for a progressively lasting warm winter), and the descending curve from right to left (i.e., LST increases for a progressively anticipated warm summer). Table 3 supports Figure 6 presenting the total  $\Delta T_w$  associated with each target period (i.e.,  $\Delta T_w$  obtained when the transition between the two reference years occurs at the end of the averaging time window, i.e., at time  $t_2$ ), as well as the relative contributions to the total  $\Delta T_w$  of different periods of the year (winter, spring and the target period itself).

The analysis of the results highlights interesting differences between the five periods, mainly due to the stratification conditions of the lake, which significantly vary during the year. Notice that the stratification during the warm year can be approximated by the evolution of  $\delta$  during 1998 shown in Figure 4 (see also the following discussion). The mean LST in June and July (Figure 6c-d) is strongly affected by the conditions that the lake experienced during the first half of the year, as can be seen by the fact that  $\Delta T_w$  shows a significant continuous increase starting from January. Thermal inertia in both



the cold (mean year) and warm (mean year + 2°C) years is always relatively large (i.e., not so small values of  $\delta$ ), and the system keeps memory of the past conditions to the extent that the previous state controls the mean LST in June and July. Thus, warmer air temperatures during winter and/or spring may induce an anticipation of the stratification, with substantial repercussions on the values of LST. In Test 5 and 6, an amplified warming of LST is observed with respect to air temperature,  $\Delta T_w$  being up to 110% and 215% of  $\Delta T_a$  (2°C), respectively in June and July (Table 3). This dramatic effect in July results from an earlier onset of strong stratification (Figure 4b), which makes LST warming much faster in the warm year than in the cold year (compare the rising limbs of 1998 and the mean year in Figure 4a). The role played by previous lake conditions is clear: warmer air temperature during the period January to June (i.e., winter and spring months in Table 3) explains around 71% of the total simulated  $\Delta T_w$  in July for Test 5 (Figure 6d). Similar considerations can be made for June, but the memory effect is even higher: warmer air temperature during the period January to May explains around 79% of total simulated  $\Delta T_w$  for Test 5. A similar analysis can be repeated for Test 6, showing that an anticipated warm period explains 86% and 74% of  $\Delta T_w$  in June and July, respectively (which correspond to the complement to 100% of the values in Figure 6d,e).

Differently, in August and September the dependence on past conditions is completely negligible (Figure 6e-f and Table 3), with the mean LST being essentially controlled by the values of air temperature observed during the target periods (73% and 75% of the total variation, respectively for the two months). The reason is that the lake is always strongly stratified from August to September, thermal inertia is reduced (causing a short historical memory of the system), and hence LST responds much faster to current air temperature modifications, thus being substantially disconnected from past thermal conditions. Consequently, air temperature decline beginning from August causes LST to decrease at a similar rate as air temperature in the warm year because of the smaller thermal inertia (i.e., stronger stratification), while the larger thermal inertia in the cold year allows the lake to retain

383 more heat with a consequent slower decrease of LST. The overall resulting effect is a weaker increase  
384 of LST compared to air temperature, being  $\Delta T_w$  equal to 80% of  $\Delta T_a$  in August, and 63% of  $\Delta T_a$  (see  
385 Table 3) in September, respectively. Analogous considerations were already discussed in Section 3.2  
386 when presenting results of Tests 1 and 2.

387 Concerning the entire JAS period, results shown in Figure 6g are coherent with those of Test 3 and 4,  
388 with the two periods January-June and JAS contributing almost equally to LST changes in summer  
389 (JAS air temperature explains 56% of total  $\Delta T_w$  for both Test 5 and 6, see Table 3). In light of the  
390 previous discussion on the contribution of the individual months, it is interesting to note that the JAS-  
391 averaged LST is affected by winter and spring conditions only because of the presence of July in the  
392 period.

393 Furthermore, the simultaneous comparison of Test 5 and 6 allows us to identify an intersection point.  
394 This represents the day of the year in which the effect of a warm winter with a cold summer is  
395 comparable to that of a cold winter with a warm summer. Considering June and July, the intersection  
396 time is located about one month before the start of the target period, while for August and September  
397 the intersection is within the period, suggesting again that in these months LST dynamics are chiefly  
398 controlled by the concurrent air temperature signal.

399 As a final note, we recall that the warm year characterized by  $T_{my} + 2^\circ\text{C}$  was chosen as an  
400 approximation of the conditions in 1998. In order to show the actual difference between the mean year  
401 and 1998, we have reported this case in Figure 5 using dashed lines (Test 5\* and Test 6\*). Neglecting  
402 small variations due to the more irregular pattern of air temperature difference, the results are  
403 essentially the same: June and July are affected by previous thermal conditions, while LST in August  
404 and September depends almost exclusively on the air temperature in that period. Interestingly, in Figure  
405 5 (subplots c, d and g) it is possible to recognize the effect of the exceptionally warm air temperature

406 values in February (nearly 6°C warmer than in the mean year, on average) on the mean LST in June,  
407 July and, to a minor extent, also on JAS.

#### 408 4. Discussion

409 Prediction of LST is crucial because it exerts a strong control on lake biogeochemistry and ecology,  
410 influencing water quality parameters, chemical reaction rates, presence of pathogens, photosynthesis by  
411 algae and aquatic plants, and the habitat for macroinvertebrates and fishes [e.g., *Wetzel*, 2001]. For  
412 instance, higher temperatures increase algal photosynthesis and the metabolic rates of most aquatic  
413 animals, thus requiring more food and oxygen, which is contrasting with the reduced oxygen flux from  
414 the atmosphere to the lake [*Winder and Sommer*, 2012]. The surface layer of lakes is indeed rich in  
415 biodiversity, and at the same is very sensitive to thermal alterations, whereas the deep waters are  
416 substantially not affected during the periods of strong stratification, which dramatically reduces the  
417 vertical fluxes across the thermocline [e.g., *Imberger*, 1998]. This isolation of the surface layer from  
418 below strengthens with stratification (larger temperature gradients) even though the epilimnion may  
419 become thicker. Thus, the reactive volume shrinks and responds more rapidly to the heat exchanged  
420 with the atmosphere. The process is governed by complex mechanisms, which are retained in our  
421 formulation only in a simplified, yet effective, way. In particular, *air2water* does not need to  
422 reconstruct the individual terms of the heat budget, nor the vertical mixing process in the water body.  
423 In its lumped formulation, it directly provides the relevant information that is LST and a metric for  
424 thermal stratification. Through the calibration phase, the model assimilates the dominant features of the  
425 examined lake, with the formulation remaining general and the parameters being specific of the case  
426 study. Interestingly, a few parameters capture the thermal behavior (for instance, the single parameter  
427  $a_4$  controls summer stratification), thus leading to a synthetic description and, potentially, to a  
428 classification of lake thermal properties (in this respect, see the attempt done in *Toffolon et al.* [2014]).

429 The simplicity and robustness of the model suggests its possible use in long-term predictions. This is  
430 particularly relevant in a future perspective, since lake temperatures are expected to be affected by  
431 warming trends as a result of climate change [e.g., *Mortsch and Quinn*, 1996; *Stefan et al.*, 1998].  
432 Some studies investigated the effect of varying meteorological forcing (including air temperature) on  
433 lake thermal dynamics by means of process-based one-, two- and three-dimensional numerical models  
434 [*Leon et al.*, 2005; *Yamashiki et al.*, 2010; *Wahl and Peeters*, 2014]. Three-dimensional (3D) models  
435 are especially designed to describe the individual processes, but require large computational times and  
436 are usually applied for short-term simulations. Moreover, they require detailed time series of  
437 meteorological data as input (e.g., wind speed, humidity, cloudiness, etc., in addition to air  
438 temperature), which are often not available or not provided with the needed time resolution.

439 In order to overcome these limitations, regression models have been widely used in climate change  
440 impact assessment [e.g., *Dokulil*, 2014], extrapolating LST from air temperature measurements on the  
441 basis of linear or nonlinear regression relationships. These models are indeed attractive because of their  
442 simplicity and limited requirement of meteorological data, but their use may be questionable in a  
443 climate change context especially when it is necessary to extrapolate temperature values beyond the  
444 limits of the measured time series.

445 In this perspective, *air2water* represents a valuable alternative tool to regression models, which require  
446 the same data in input but are not able to address some fundamental processes (e.g., the hysteresis cycle  
447 between air and water temperature). Furthermore, it can be used in place of process-based models when  
448 meteorological data are not sufficient for a proper calibration during a reference climate scenario. In  
449 this respect, we note that downscaling climate projections from the coarse resolution of the climate  
450 models to a finer scale suitable for the predictive lake model is a complex issue. In order to apply the  
451 downscaling procedure, a significantly large amount of historical data is required for all the

452 meteorological forcing, with the drawback that the downscaling of some variables (especially  
453 precipitation, cloudiness, wind and radiative fluxes) is usually associated with large uncertainties [e.g.,  
454 *Dettinger*, 2013]. Differently, *air2water* requires as an input variable a quantity whose downscaling  
455 procedure is very robust, i.e. air temperature, and thus can be seen as a valuable tool in climate change  
456 impact studies, allowing for predictions of future trends of lake surface water temperature. Finally, the  
457 possibility of coupling *air2water*, as a lumped lake model, in atmospheric circulation and weather  
458 prediction models has also been evidenced by *Toffolon et al.*, [2014].

## 459 5. Conclusions

460 The present analysis contributes to the understanding of the conditions leading to extreme warming of  
461 lake surface temperature (LST). These events typically occur for a positive combination of two factors:  
462 i) warm winter and spring seasons anticipate the onset of direct stratification, thus reducing the volume  
463 (and hence the thermal inertia) of the lake surface layer; ii) with a relatively thin layer reacting to the  
464 surface heat flux, a warm summer season can determine a pronounced warming of LST, which rapidly  
465 adapts to air temperature conditions in July, August and September (JAS). Such a description is  
466 confirmed by the analysis of the exceptional warming of Lake Superior in summer 1998, which was  
467 determined by the concurrence of both factors.

468 The *air2water* model was shown to be able to capture the positive feedback between LST and  
469 stratification. Therefore, we analyzed some synthetic scenarios in order to isolate the relative  
470 contributions of the different factors, showing that the increase of LST during summer 1998 is almost  
471 equally imputable to what happened in January-June (and hence to the stratification conditions at the  
472 beginning of the considered period) and to air temperature in JAS. This result is in line with *Austin and*  
473 *Colman* [2007] who based their analysis on a different method relying on long-term trends. The model  
474 also suggests that July is the month where the increase of LST with respect to a warmer air temperature

475 is maximum, and strongly dependent upon the previous months, while LST in August and September is  
476 affected only by concurrent air temperature. Given that the JAS period is often considered in statistical  
477 analyses of Lake Superior, our results suggest the opportunity to use a more appropriate index to  
478 characterize the changes in the thermal behavior of the lake in summer. In this respect, we recommend  
479 future analyses to separate the contribution of the different summer months on the averaged warming,  
480 since the mechanisms that control LST in July are inherently different from those in August and  
481 September.

482 As a whole, the results point out that the dynamics of thermal stratification of the lake are crucial for  
483 the seasonal evolution of surface water temperature, and should be carefully considered in this kind of  
484 analyses. In this regard, despite the simplicity of the model, we demonstrated that it is able to  
485 satisfactorily reproduce the main processes controlling the response of LST, and can be effectively  
486 used to perform sensitivity analyses aimed at evaluating the role exerted by air temperature in  
487 controlling the seasonal behavior of stratification and LST. This possibility is especially relevant in  
488 climate change studies, where the scenarios for water temperature (when available) contain much more  
489 uncertainties than those for air temperature. Thus, *air2water* may contribute to reconstruct first  
490 approximations of the future dynamics of LST as one of the main drivers of ecology and  
491 biogeochemistry in lentic waters.

## 492 **Appendix A: Net heat flux at the lake-atmosphere interface**

493 The net heat flux per unit surface  $\Phi_{net}$  in equation (1) can be decomposed in the following terms  
494 (defined as positive when directed to the lake surface layer):

$$495 \quad \Phi_{net} = \Phi_S + \Phi_A + \Phi_W + \Phi_L + \Phi_C + \Phi_P + \Phi_I + \Phi_D , \quad (A1)$$

where  $\Phi_S$  is the net short-wave solar radiation actually absorbed by the water volume,  $\Phi_A$  is the net long-wave radiation emitted from the atmosphere towards the river,  $\Phi_W$  is the long-wave radiation emitted from the water,  $\Phi_L$  is the latent heat flux due to evaporation/condensation,  $\Phi_C$  is the sensible heat flux due to convection,  $\Phi_P$  is the heat flux due to precipitation,  $\Phi_I$  is the effect of the throughflow by inlets and outlets, and  $\Phi_D$  is the heat flux exchanged with deep water.

Following *Piccolroaz et al.*, [2013], which the reader is referred to for further details, we linearize all the terms composing  $\Phi_{net}$  as a function of  $T_w$  and  $T_a$  as follows:

$$\Phi = \Phi_0 + \left. \frac{\partial \Phi}{\partial T_a} \right|_{T_{a0}} (T_a - T_{a0}) + \left. \frac{\partial \Phi}{\partial T_w} \right|_{T_{w0}} (T_w - T_{w0}), \quad (\text{A2})$$

where  $\Phi$  is a generic flux term present in (A1),  $T_{w0}$  and  $T_{a0}$  are reference values (e.g., long-term averages) of LST and air temperature, respectively, and  $\Phi_0$  is the part of the heat flux that is independent of variation of air and water temperatures, but that can vary in time. We further assume that, for the purposes of the present analysis, the term  $\Phi_0 + \left. \frac{\partial \Phi}{\partial T_a} \right|_{T_{a0}} + \left. \frac{\partial \Phi}{\partial T_w} \right|_{T_{w0}}$  can be approximately described by the sum of a constant value and a sinusoidal function of time with a period of one year.

Hence, substituting (A1) and (A2) into equation (1) we obtain:

$$\frac{dT_w}{dt} = \frac{A}{\rho c_p V_s} (\hat{a}_1 + \hat{a}_2 T_a - \hat{a}_3 T_w + \hat{a}_t), \quad (\text{A3})$$

where  $\hat{a}_1$ ,  $\hat{a}_2$  and  $\hat{a}_3$  are coefficients that can be directly derived by the heat flux terms once suitable empirical relationships are adopted [e.g., *Martin and McCutcheon*, 1998], and  $\hat{a}_t$  is the sinusoidal term. We also introduce the dimensionless ratio  $\delta = V_s/V_r$ , where the reference volume  $V_r$  is left unspecified. Thus, equation (A3) can be rewritten as:

$$\frac{dT_w}{dt} = \frac{V_r}{V_s} \left( \frac{A \hat{a}_1}{\rho c_p V_r} + \frac{A \hat{a}_2}{\rho c_p V_r} T_a - \frac{A \hat{a}_3}{\rho c_p V_r} T_w + \frac{A \hat{a}_t}{\rho c_p V_r} \right), \quad (\text{A4})$$

516 which it is straightforward to reformulate as in equation (2) by introducing  $\delta$  and the parameters  $a_1$ ,  $a_2$ ,  
517  $a_3$ ,  $a_5$  and  $a_6$ .

518 In order to account for the strong seasonal variations of the reactive layer volume, we assume that  $\delta$  is  
519 a function of the difference between LST and the deep water temperature  $T_h$  as specified in equation  
520 (3), with the introduction of three additional parameters:  $a_4$  to quantify the effect of direct  
521 stratification, and  $a_7$  and  $a_8$  to account for inverse stratification and the effect of ice cover (we impose  
522  $T_w \geq 0$  as a lower limit for simulated LST).

523 Finally, we note that the last two terms of equation (A1) are not explicitly considered in the analysis,  
524 but their effect is implicitly retained by the other parameters through the calibration procedure. We  
525 refer to *Toffolon et al.*, [2014] for a more extensive discussion of the physical interpretation of the  
526 parameters.

527

## 528 **Acknowledgements**

529 The authors are grateful to NOAA (National Oceanic and Atmospheric Administration) for air  
530 temperature and LST data used in this work (data can be downloaded from  
531 <http://www.ndbc.noaa.gov/>). Authors are indebted to Jay Austin for kindly providing vertical  
532 temperature profiles (National Science Foundation grant OCE-0825633), and for the helpful comments  
533 and contribution. We also thank Michael Notaro for the discussion during the early stage of the work,  
534 and the three anonymous Reviewers for their valuable suggestions.



535   **References**

- 536   Adrian, R., C. M. O'Reilly, H. Zagarese, S. B. Baines, D. O. Hessen, W. Keller, D. M. Livingstone, R.  
537   Sommaruga, D. Straile, E. V. Donk, G. A. Weyhenmeyer, M., and Winder (2009), Lakes as sentinels of  
538   climate change, *Limnol. Oceanogr.*, 54(6 part 2), 2283–2297, DOI: 10.4319/lo.2009.54.6\_part\_2.2283
- 539   Anderson, W.L., D.M. Robertson, and J.J. Magnuson (1996), Evidence of recent warming and El Nino-  
540   related variation in ice breakup of Wisconsin lakes, *Limnol. Oceanogr.*, 41(5), 815–821
- 541   Assel, R. A., J. E. Janowiak, D. Boyce, C. O'Connors, F. H. Quinn, and D. C. Norton (2000),  
542   Laurentian Great Lakes Ice and Weather Conditions for the 1998 El Niño Winter, *Bull. Amer. Meteor.*  
543   *Soc.*, 81, 703–717, DOI: [http://dx.doi.org/10.1175/1520-0477\(2000\)081<0703:LGLIAW>2.3.CO;2](http://dx.doi.org/10.1175/1520-0477(2000)081<0703:LGLIAW>2.3.CO;2)
- 544   Austin, J. A., and S. M. Colman (2007), Lake Superior summer water temperatures are increasing more  
545   rapidly than regional air temperatures: a positive ice-albedo feedback, *Geophys. Res. Lett.*, 34(6),  
546   DOI: 10.1029/2006GL029021
- 547   Austin, J. A., and S. M. Colman (2008), A century of temperature variability in Lake Superior, *Limnol.*  
548   *Oceanogr.*, 53(6), 2724–2730, DOI: 10.4319/lo.2008.53.6.2724
- 549   Blanken, P. D., C. Spence, N. Hedstrom, and J. D. Lenters (2011), Evaporation from Lake Superior: 1.  
550   Physical controls and processes, *J. Great Lakes Res.*, 37(4), DOI: 10.1016/j.jglr.2011.08.009
- 551   Cline T.J., V. Bennington, and J. F. Kitchell (2013), Climate Change Expands the Spatial Extent and  
552   Duration of Preferred Thermal Habitat for Lake Superior Fishes, *PLoS ONE*, 8(4), DOI:  
553   10.1371/journal.pone.0062279
- 554   Coats, R., J. Perez-Losada, G. Schladow, R. Richards, and C. Goldman (2006), The warming of Lake  
555   Tahoe, *Climatic Change*, 76(1–2), 121–148, DOI: 10.1007/s10584-005-9006-1

556 De Senerpont Domis, L. N., J.J. Elser, A.S. Gsell, V.L.M. Huszar, B.W. Ibelings, E. Jeppesen, S.  
 557 Kosten, W.M. Mooij, F. Roland, U. Sommer, E. Van Donk, M. Winder, and M. Lürling, (2013),  
 558 Plankton dynamics under different climatic conditions in space and time, *Freshw. Biol.*, 58, 463–482,  
 559 doi:10.1111/fwb.12053

560 Dettinger, M. (2013), Projections and downscaling of 21st century temperatures, precipitation, radiative  
 561 fluxes and winds for the Southwestern US, with focus on Lake Tahoe, *Climatic Change*, 116, 17-33.

562 Dokulil, M. T. (2014), Predicting summer surface water temperatures for large Austrian lakes in 2050  
 563 under climate change scenarios, *Hydrobiologia*, 731, 19–29, DOI: 10.1007/s10750-013-1550-5

564 Gupta H. V., H. Kling, K. K. Yilmaz, and G. F. Martinez (2009), Decomposition of the mean squared  
 565 error and NSE performance criteria: Implications for improving hydrological modelling, *J. Hydrol.*,  
 566 377(1-2), 80-91, DOI: 10.1016/j.jhydrol.2009.08.003

567 Hampton, S. E., L. R. Izmet'seva, M. V. Moore, S. L. Katz, B. Dennis, and E. A. Silow (2008), Sixty  
 568 years of environmental change in the world's largest freshwater lake – Lake Baikal, Siberia, *Glob.*  
 569 *Change Biol.*, 14(8), 1947-1958, DOI: 10.1111/j.1365-2486.2008.01616.x

570 Imberger, J, ed. (1998), Physical Processes in Lakes and Oceans, Coastal Estuarine Stud. 54,  
 571 Washington, DC, Am. Geophys. Union.

572 Lenters, J. D. (2004), Trends in the Lake Superior water budget since 1948: A weakening seasonal  
 573 cycle, *J. Gt. Lakes Res.*, 30(Supplement 1) 20-40, DOI: 10.1016/S0380-1330(04)70375-5

574 Lenters, J. D., S. J. Hook, and P. B. McIntyre (2012), Workshop examines warming of lakes  
 575 worldwide, *Eos T. Am. Geophys. Un.*, 93(43), 427, DOI:10.1029/2012EO430004.

576 Leon, L. F., D. C. L. Lam, W. Schertzer and D. Swayne (2005), Lake and climate models linkage: A 3-  
577 D hydrodynamic contribution, *Adv. Geosci.* 4, 57–62, DOI:10.5194/adgeo-4-57-2005.

578 Livingstone, D. M. (2003), Impact of secular climate change on the thermal structure of a large  
579 temperate central European lake, *Climatic Change*, 57(1–2), 205–225, DOI:  
580 10.1023/A:1022119503144

581 Lofgren, B. M., and Y. Zhu (1999), Seasonal climatology of surface energy fluxes on the Great Lakes,  
582 NOAA technical memorandum ERL GLERL, 112, NOAA

583 Magnuson, J. J., K. E. Webster K.E., R. A. Assel, C. J. Bowser, P. J. Dillon, J. G. Eaton, H. E. Evans,  
584 E. J. Fee, L. D. Mortsch, D. W. Schindler, and F. H. Quinn (1997), Potential effects of climate changes  
585 on aquatic systems: Laurentian Great Lakes and Precambrian Shield region, *Hydrol. Processes*, 11(8),  
586 825– 871, DOI: 10.1002/(SICI)1099-1085(19970630)11:8<825::AID-HYP509>3.0.CO;2-G

587 Martin, J. L., and S. McCutcheon (1998), Hydrodynamics and Transport for Water Quality Modeling,  
588 CRC Press.

589 McCormick, M. J., and G. L. Fahnenstiel (1999), Recent climatic trends in nearshore water  
590 temperatures in the St. Lawrence Great Lakes, *Limnol. Oceanogr.*, 44(3), 530-540, DOI:  
591 10.4319/lo.1999.44.3.0530

592 Mortsch, L. D., and F. H. Quinn (1996), Climate change scenarios for Great Lakes Basin ecosystem  
593 studies, *Limnol. Oceanogr.*, 41(5), 903-911.

594 Piccolroaz, S., M. Toffolon, and B. Majone (2013), A simple lumped model to convert air temperature  
595 into surface water temperature in lakes, *Hydrol. Earth Syst. Sci.*, 17, 3323-3338, DOI: 10.5194/hess-17-  
596 3323-2013

597 Quayle, W., L. Peck, H. Peat, J. Ellis-Evans, and P. Harrigan (2002), Extreme responses to climate  
 598 change in Antarctic lakes, *Science*, 295(5555), 645, DOI: 10.1126/science.106407

599 Schindler, D.W., S.E. Bayley, B.R. Parker, K.G. Beaty, D.R. Cruikshank, E.J. Fee, E.U. Schindler, and  
 600 M.P. Stainton (1996), The effects of climatic warming on the properties of boreal lakes and streams at  
 601 the Experimental Lakes Area, northwestern Ontario, *Limnol. Oceanogr.*, 41(5), 1004–1017

602 Schneider, P., S. J. Hook, R. G. Radocinski, G. K. Corlett, G. C. Hulley, S. G. Schladow, and T. E.  
 603 Steissberg (2009), Satellite observations indicate rapid warming trend for lakes in California and  
 604 Nevada, *Geophys. Res. Lett.*, 36(22), DOI: 10.1029/2009GL040846

605 Schneider, P., and S. J. Hook (2010), Space observations of inland water bodies show rapid surface  
 606 warming since 1985, *Geophys. Res. Lett.*, 37(22), DOI: 10.1029/2010GL045059

607 Schwab, B. J., G. A. Leshkevich, and G. C. Muhr (1999), Automated Mapping of Surface Water  
 608 Temperature in the Great Lakes, *J. Great Lakes Res.*, 25(3), 468-481, DOI:10.1016/S0380-  
 609 1330(99)70755-0

610 Stefan, H. G., X. Fang, and M. Hondzo (1998), Simulated climate change effects on year-round water  
 611 temperatures in temperate zone lakes, *Climatic Change*, 40, 547–576. Thiery, W., V. M. Stepanenko, X.  
 612 Fang, K. D. Jöhnk, Z. Li, A. Martynov, M. Perroud, Z. M. Subin, F. Darchambeau, D. Mironov, and N.  
 613 P. M. Van Lipzig (2014), LakeMIP Kivu: Evaluating the representation of a large, deep tropical lake by  
 614 a set of one-dimensional lake models, *Tellus A*, 66(1), 1-18, DOI:10.3402/tellusa.v66.21390

615 Thiery, W., V. M. Stepanenko, X. Fang, K. D. Jöhnk, Z. Li, A. Martynov, M. Perroud, Z. M. Subin, F.  
 616 Darchambeau, D. Mironov, and N. P. M. van Lipzig (2014), LakeMIP Kivu: Evaluating the  
 617 representation of a large, deep tropical lake by a set of 1-dimensional lake models, *Tellus A*, 66, 21390,  
 618 <http://dx.doi.org/10.3402/tellusa.v66.21390>

619 Titze, D. D., and J. A. Austin (2014), Winter Thermal Structure of Lake Superior, *Limnol. Oceanogr.*,  
620 59(4), 1336-1348, DOI:10.4319/lo.2014.59.4.1336

621 Toffolon, M., S. Piccolroaz, B. Majone, A.-M. Soja, F. Peeters, M. Schmid, and A. Wüest (2014),  
622 Prediction of surface temperature in lakes with different morphology using air temperature, *Limnol.*  
623 *Oceanogr.*, 59(6), 2185-2202, DOI:10.4319/lo.2014.59.6.2185

624 Van Cleave, K., J. D. Lenters, J. Wang, and E. M. Verhamme (2014), A regime shift in Lake Superior  
625 ice cover, evaporation, and water temperature following the warm El Niño winter of 1997–1998,  
626 *Limnol. Oceanogr.*, 59(6), 1889-1898, DOI: 10.4319/lo.2014.59.6.1889

627 Verburg, P., R. E. Hecky, and H. Kling (2003), Ecological consequences of a century of warming in  
628 Lake Tanganyika, *Science*, 301(5632), 505–507, DOI: 10.1126/science.1084846

629 Vollmer, M. J., H. A. Bootsma, R. E. Hecky, G. Patterson, J. D. Halfman, J. M. Edmond, D. H. Eccles,  
630 and R. F. Weiss (2005), Deep – water warming trend in Lake Malawi, East Africa, *Limnol. Oceanogr.*,  
631 50(2), 727–732, DOI: 10.4319/lo.2005.50.2.0727

632 Wahl, B., and F. Peeters (2014), Effect of climatic changes on stratification and deep-water renewal in  
633 Lake Constance assessed by sensitivity studies with a 3D hydrodynamic model, *Limnol. Oceanogr.*, 59:  
634 1035–1052, DOI:10.4319/lo.2014.59.3.1035

635 Wetzel, R. G. (2001), *Limnology: Lake and River Ecosystems*, Academic Press, San Diego, 3rd Edn.

636 Williamson, C. E., J. E. Saros, W. F. Vincent, and J. P. Smol (2009), Lakes and reservoirs as sentinels,  
637 integrators, and regulators of climate change, *Limnol. Oceanogr.*, 54(6 part 2), 2273–2282, DOI:  
638 10.4319/lo.2009.54.6\_part\_2.2273

639 Winder, M., and U. Sommer (2012), Phytoplankton response to a changing climate. *Hydrobiologia*,  
640 698, 5–16, doi:10.1007/s10750-012-1149-2

641 Yamashiki, Y., M. Kato, K. Takara, E. Nakakita and M. Kumagai (2010), Sensitivity Analysis on Lake  
642 Biwa under the A1B SRES climate change scenario using Biwa-3D Integrated Assessment Model: part  
643 I – projection of lake temperature, *Hydrological Research Letters*, 4, 45–49, DOI: 10.3178/HRL.4.45

644 **Tables**

645 Table 1: Synthetic scenarios obtained combining different periods of air temperature and choosing  
646 different procedures for estimating the volume ratio  $\delta$ .

Scenario	$T_a$	$\delta$
Test 1 ( $T_a$ 1998 & $\delta$ 1997)	1998	1997
Test 2 ( $T_a$ 1997 & $\delta$ 1998)	1997	1998
Test 3 (steeper $T_a$ )	1997: Oct-Jun 1998: Jul-Aug	Model
Test 4 (flatter $T_a$ )	1998: Oct-Jun 1997: Jul-Aug	Model
Test 5 (ensemble of 365 cases) (lasting warm winter)	$T_{my}+2^{\circ}\text{C}$ : DOY=1,i <sup>a</sup> $T_{my}$ : DOY=i+1,365	Model
Test 6 (ensemble of 365 cases) (anticipated warm summer)	$T_{my}$ : DOY=1,i $T_{my}+2^{\circ}\text{C}$ : DOY=i+1,365	Model
Test 5* (ensemble of 365 cases) (lasting warm winter)	1998: DOY=1,i $T_{my}$ : DOY=i+1,365	Model
Test 6* (ensemble of 365 cases) (anticipated warm summer)	$T_{my}$ : DOY=1,i 1998: DOY=i+1,365	Model

647 <sup>a</sup> DOY stands for day of the year

649 Table 2: Simulated annual maximum, mean summer (JAS) and mean monthly (June, July, August and  
650 September, respectively) LST for years 1997 and 1998, and for the synthetic scenarios Test 1-4  
651 reported in Table 1.

Cases	1997	1998	Test 1	Test 2	Test 3	Test 4
	$T_w$ [°C]					
Period						
maximum	15.17	19.14	17.61	17.25	18.76	16.55
JAS	11.97	16.19	14.48	13.61	14.58	13.63
Jul	8.65	15.50	10.76	12.86	10.62	12.67
Aug	14.02	17.69	16.81	14.77	17.55	14.88
Sep	13.28	15.35	15.73	13.10	15.35	13.30



653 Table 3: Period-averaged LST difference between the synthetic year and the mean year for Test 5 and  
 654 Test 6, respectively, considering different target periods (i.e., June, July, August, September and JAS).  
 655 The separate effects associated to winter and spring seasons and that of the target period are also  
 656 reported.

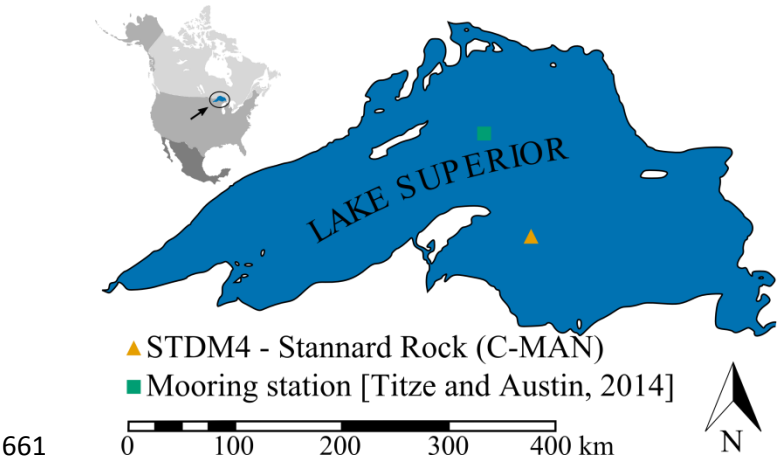
		Winter (JFM <sup>a</sup> )	Spring (AMJ <sup>b</sup> )	Target period	Total
Target period	Test	$\Delta T_w$ [°C] (referred to the mean of the target period)			
Jun	5	0.67	1.05 <sup>c</sup>	0.47	2.19
		(30.4%)	(48.1%)	(21.5%)	
	6	0.88	1.00 <sup>c</sup>	0.31	
		(40.1%)	(45.9%)	(14.0%)	
Jul	5	0.96	2.10	1.25	4.31
		(22.2%)	(48.8%)	(29.0%)	
	6	0.80	2.37	1.13	
		(18.7 %)	(55.0%)	(26.3%)	
Aug	5	0.08	0.07	1.18	1.62
		(5.1%)	(4.1%)	(73.0%)	
	6	<0.01	0.03	1.18	
		(0.1%)	(2.0%)	(72.9%)	

Sep	5	0.00	0.00	0.96	1.27	
		(0.0%)	(0.0%)	(75.3%)		
	<hr/>					
	6	0.00	0.00	0.95		
(0.0%)		(0.0%)	(75.0%)			
<hr/>						
JAS	5	0.34	0.70	1.34	2.38	
		(14.3%)	(29.4%)	(56.3%)		
	<hr/>					
	6	0.26	0.78	1.34		
(10.8%)		(32.9%)	(56.3%)			

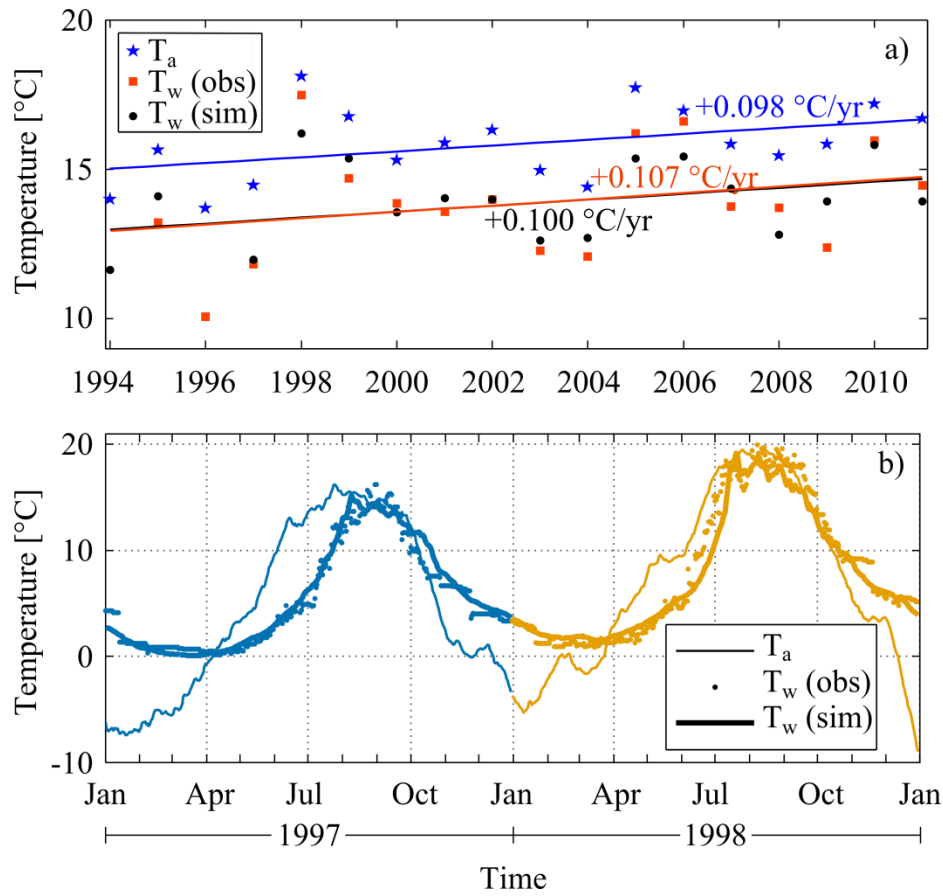
657    <sup>a</sup> January, February and March

658    <sup>b</sup> April, May and June

659    <sup>c</sup> For the case of June spring months are only April and May (AM).



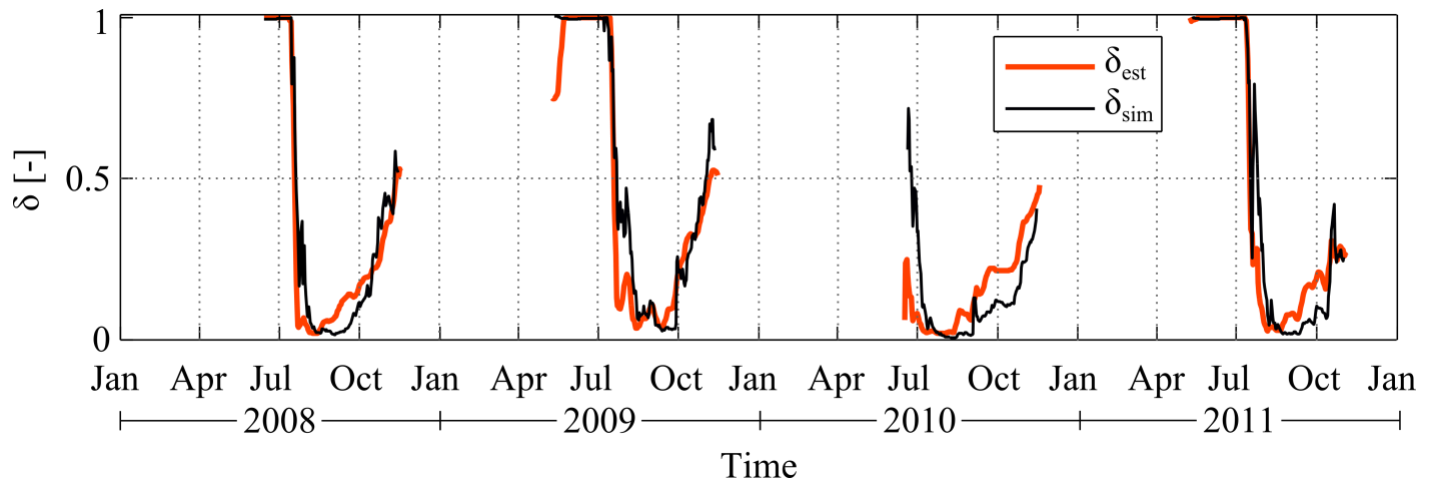
662 Figure 1: Lake Superior with the location of the air temperature station (STD4 – Stannard Rock) and  
663 the moored thermistor chain [Titze and Austin, 2014] used in this work.



664

665 Figure 2: Comparison between air temperature  $T_a$  (observed) and lake surface temperature  $T_w$   
 666 (observed and simulated): (a) long-term trends of mean summer values (JAS) within the period 1994-  
 667 2011; and (b) daily values in 1997 and 1998. LST is retrieved by satellite imagery (GLERL dataset).  
 668 For representation purposes, air temperature has been filtered with a 30 days moving average in (b).

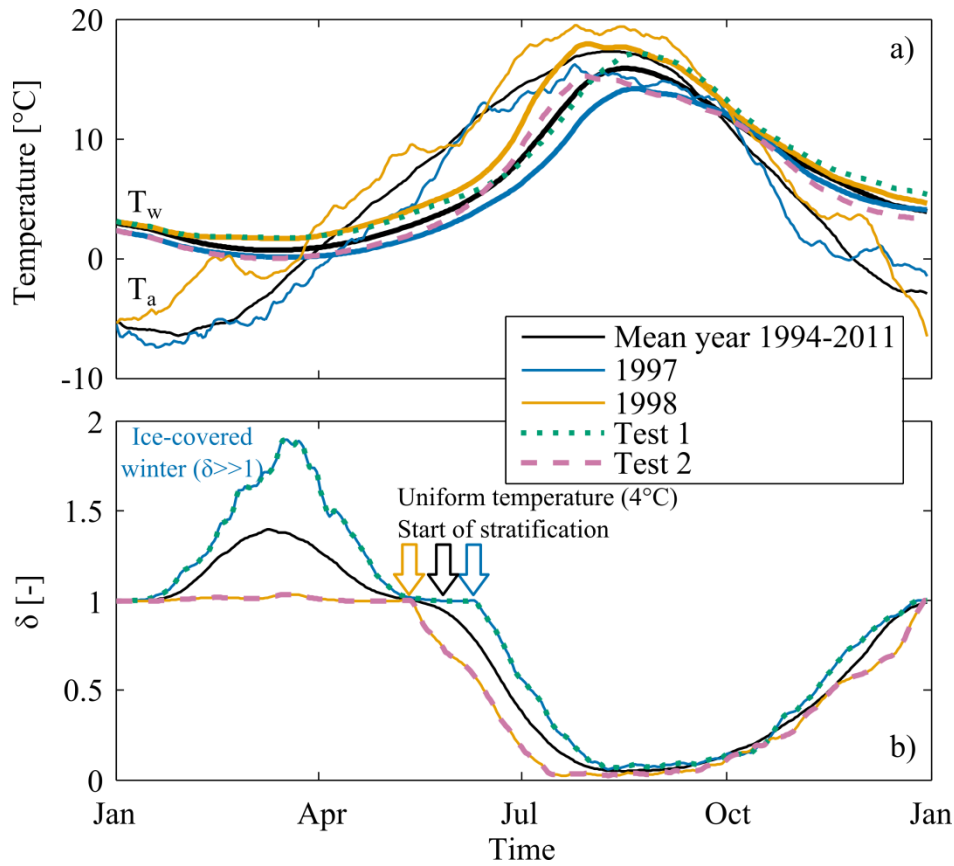
669



670

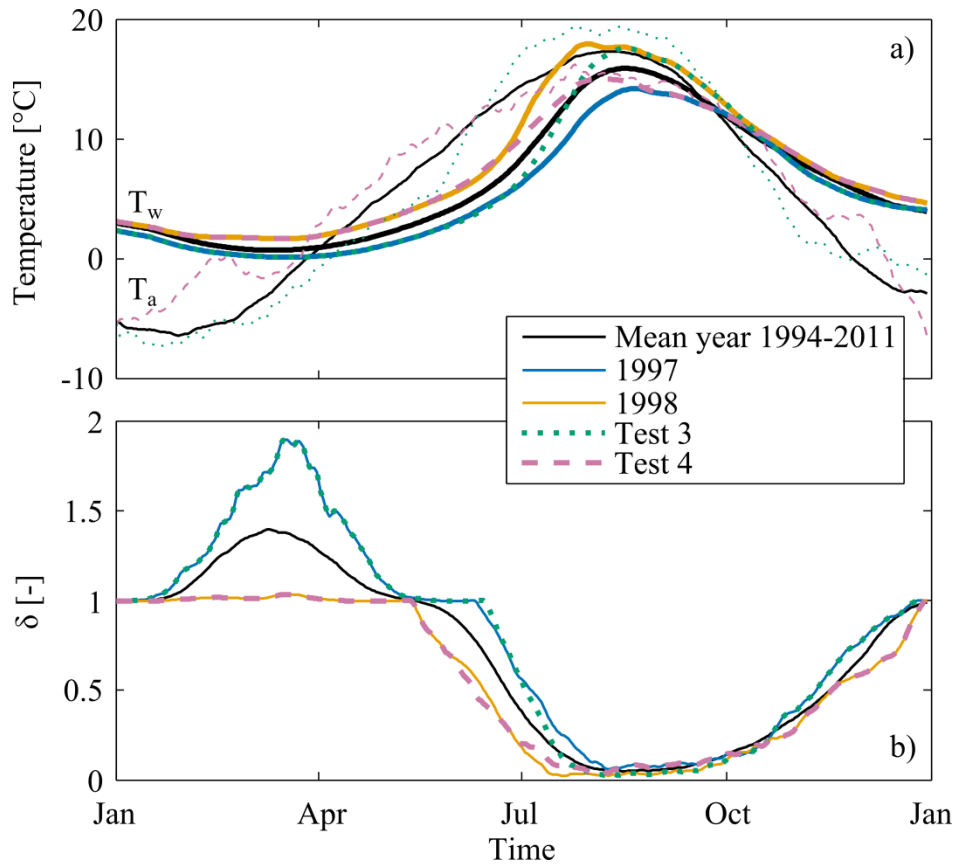
671 Figure 3: Comparison between  $\delta$  simulated by *air2water* ( $\delta_{sim}$ ) and estimated from the analysis of  
 672 water temperature profiles measured at the mooring station indicated in Figure 1 ( $\delta_{est}$ ). For  
 673 representation purposes  $\delta_{est}$  has been filtered with a 7 days moving average.

674



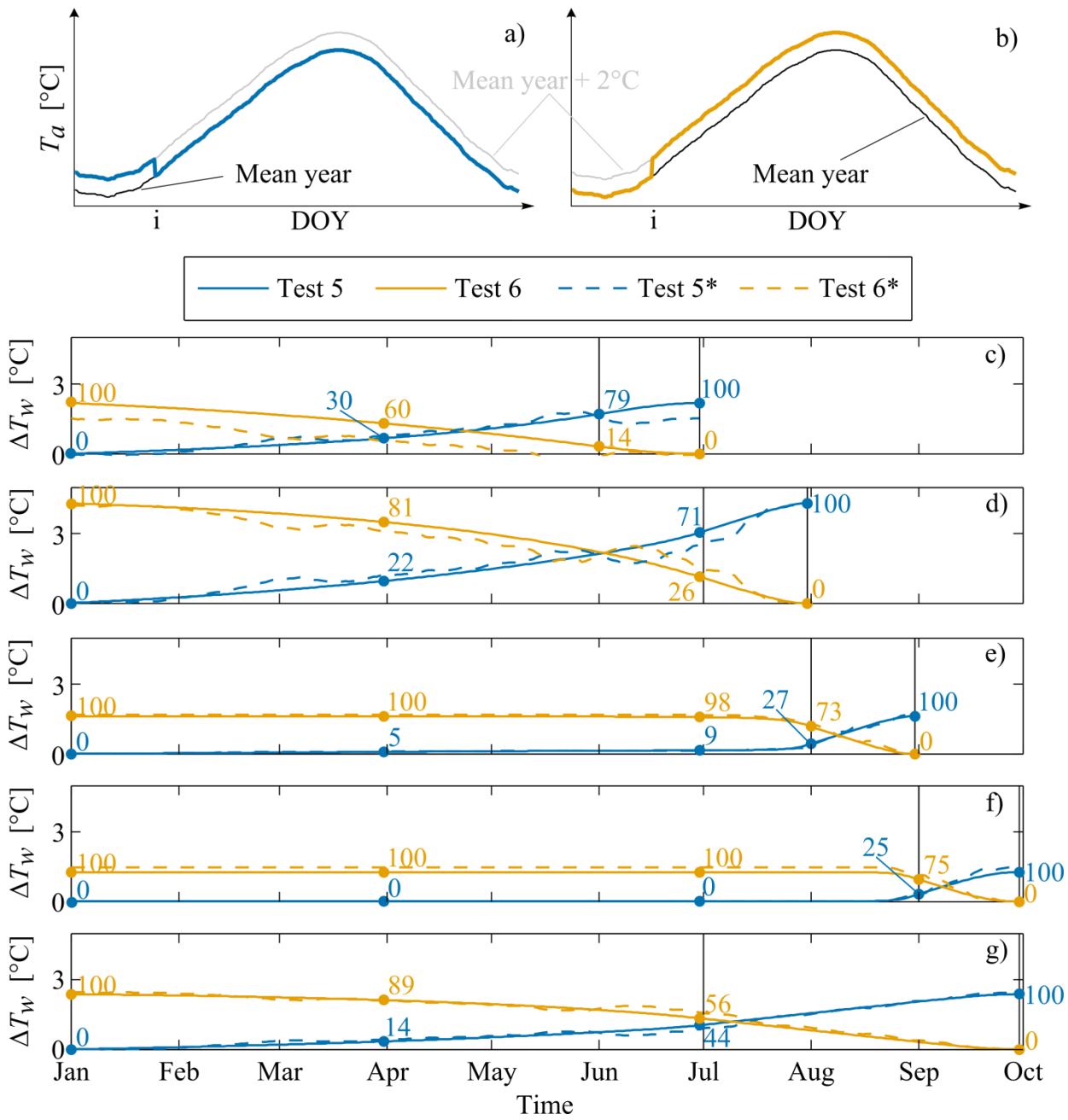
675

676 Figure 4: Annual cycle of (a) observed  $T_a$  (thin line) and simulated  $T_w$  (thick line), and (b) volume ratio  
 677  $\delta$ , considering 1997, 1998, mean year 1994-2011, Test 1 (dotted line), and Test 2 (dashed line). The  
 678 value of  $\delta$  is imposed in the two tests (see Table 1). For representation purposes, all temperature series  
 679 have been filtered with a 30 days moving average.



680

681 Figure 5: Annual cycle of (a) reconstructed  $T_a$  (thin line, see Table 1) and simulated  $T_w$  (thick line), and  
 682 (b) simulated volume ratio  $\delta$ , considering 1997, 1998, mean year 1994-2011, Test 3 (dotted line), and  
 683 Test 4 (dashed line). The value of  $\delta$  is calculated in all cases. For representation purposes, all  
 684 temperature series have been filtered with a 30 days moving average.



685

686

687

688

689

690

Figure 6: Analysis of Test 5 and Test 6, composed by a set of cases depending on the day of the year (DOI) where the transition occurs (see Table 1): (a) reconstructed  $T_a$  for Test 5 and (b) for Test 6, for a given day  $i$ ; (c)-(g) period-averaged LST difference  $\Delta T_w$  as a function of  $i$  (vertical lines denote the limit of the period considered for averaging: June, July, August, September and JAS, respectively from subplot c to subplot g).